RNA binding and thiolytic stability of a quinoline-containing helix-threading peptide

Malathy Krishnamurthy, Barry D. Gooch and Peter A. Beal*

Received (in Pittsburgh, PA, USA) 28th September 2005, Accepted 22nd December 2005
First published as an Advance Article on the web 24th January 2006
DOI: 10.1039/b513591e

Helix-threading peptides (HTPs) bind selectively to sites predisposed to intercalation in folded RNA molecules placing peptide functional groups into the dissimilar grooves of the duplex. Here we report the design and synthesis of new HTPs with quinoline as the intercalation domain. A quinoline-containing HTP is shown to bind selectively to duplex RNA binding sites. Furthermore, the affinity cleavage pattern generated using an EDTA·Fe modified derivative is consistent with minor groove localization of its *N*-terminus. This compound binds base-pair steps flanked by single nucleotide bulges on the 3′ side on both strands, whereas bulges on the 5′ side of the intercalation site do not support binding. Furthermore, unlike acridine HTPs, the quinoline compound is resistant to thiolytic degradation that leads to loss of RNA-binding activity. The RNA-binding selectivity and stability observed for quinoline-containing HTPs make them excellent candidates for further development as regulators of intracellular RNA function.

Introduction

The design and synthesis of new RNA-binding small molecules with the ability to discriminate target over other nucleic acids inside living cells is an important step in the development of new therapeutics.[1] However, while it is clear that π-stacking and charge–charge interactions are key forces that drive the binding of small molecules to RNA, balancing these forces and combining them with directional hydrogen bonding and/or van der Waals contacts to achieve *selective* binding to predetermined RNA targets is a challenging task.[2] Our laboratory has developed helix-threading peptides (HTPs) that target duplex RNA structures selectively by threading intercalation.[3,5] These compounds bind to sites predisposed to intercalation in folded RNA molecules and project peptide functional groups into the dissimilar RNA duplex grooves. Manipulation of recognition elements present in the groove-localized domains influences the affinity of these compounds for RNA targets. Our original HTP design used 9-anilinoacridines in the intercalation domains.[3,4,9,10] However, the ability of the fused, three-ring acridine system to engage in π-stacking at off-target sites and the lability of the (acridine C9)–(aniline N) bond under biologically relevant conditions led us to investigate alternative intercalation domains for HTPs.[5] Here we describe a new HTP design that uses quinoline for intercalation. A high yielding synthesis to a new quinoline amino acid is reported along with RNA-binding properties and stabilities of quinoline-containing HTPs.

Results and discussion

Although acridine HTPs and 2-phenylquinoline HTPs have demonstrated promising selectivity in RNA binding experiments, we questioned whether the three-ring intercalator (fused or appended) was necessary or if a two-ring system would be sufficient for supporting threading into duplex RNA.[6] This design would have the advantage of reducing nonselective binding by partial intercalation at off-target sites. In an effort to prepare HTPs with such a "minimal" intercalation domain,[6] we generated an Alloc-protected 4-,8-disubstituted quinoline amino acid (Scheme 1). Initially, Meldrum's acid was condensed with methyl anthranilate and ethyl orthoformate to yield **1**.[7] Thermal cyclization of **1** generated **2** in excellent yield.[8] This compound was brominated at the 4-position to give **3** and substituted with an Alloc-protected diamine to yield fully protected amino acid **4**. Saponification of the methyl ester provided amino acid **5** ready for solid phase synthesis. This amino acid was used to generate the peptide AbuSV*Quin*R (**6**), where Abu refers to aminobutyric acid and *Quin* is the 4-(4′-methylaminoanilino)-quinoline-8-carboxylic acid (Fig. 1). Importantly, ribonuclease V1 footprinting indicated that **6** binds an HTP-binding RNA (RNA **A**) at the site occupied by other related peptides with a $K_D = 3.3 \pm 1.8$ μM (Fig. 2).[5,9] Thus, selective binding is maintained with a two-ring threading intercalator, albeit at a reduced affinity compared to acridine ($K_D = 21$ nM)[9] or 2-phenylquinoline ($K_D = 200$ nM)[5] derivatives.

The experiments discussed above indicated that a quinoline-containing HTP could be prepared that selectively binds RNA at a site predisposed to intercalation. However, the groove location of the termini could not be determined from the footprinting data alone. For the HTP SV*Acr*R, where *Acr* is our 9-(4′-methylaminoanilino)-acridine-4-carboxylic acid, the *N*-terminus lies in the minor groove and the *C*-terminus in the major groove at the binding site in RNA **A**.[4] This binding polarity is maintained for a different acridine HTP that binds a bacterial ribosomal RNA target.[10] We addressed the issue of binding polarity for the quinoline HTP by preparing EDTA·Fe–SV*Quin*R (**8**) and using the affinity cleaving method to evaluate binding on RNA **A**.[4,11] The results were compared to those generated with

Department of Chemistry, University of Utah, 315 South 1400 East, Salt Lake City, Utah, USA 84112-0850. E-mail: beal@chem.utah.edu; Fax: +1 801 581 8433; Tel: +1 801 585 9719

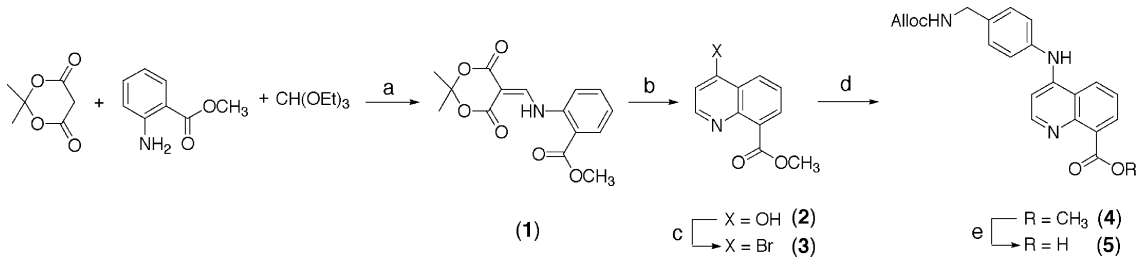

Scheme 1 Conditions and yields; (a) 70–80 °C, 45 min, 94%; (b) Ph_2O, 255 °C, 30 min, 84%; (c) PPh_3, NBS, CH_3CN, reflux, 30 min, 76%; (d) Allyl 4-aminobenzyl aminocarbamate,[3] CH_3CN, reflux, 40 min, 89%; (e) $LiOH{\cdot}H_2O$, THF–H_2O, rt, 2 h, 83%.

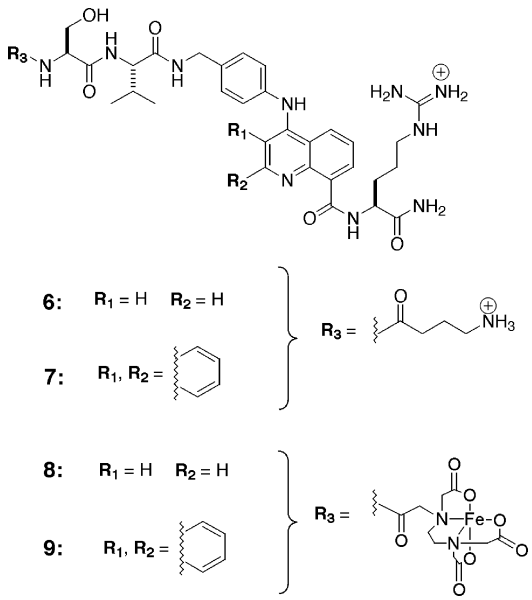

Fig. 1 Structures of helix threading peptides (HTPs) studied in this work.

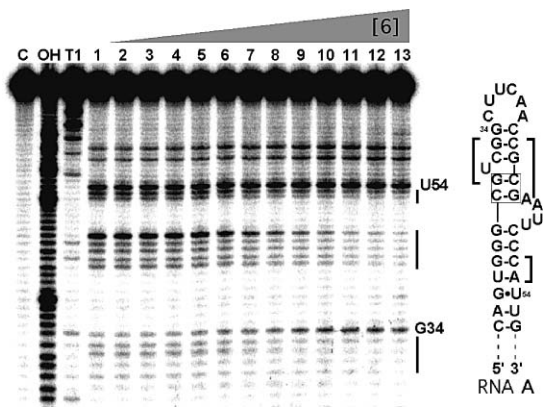

Fig. 2 Quantitative ribonuclease V1 footprinting analysis of HTP **6** binding to RNA **A**. (Left) Autoradiogram of polyacrylamide gel used to resolve footprinting reactions. Lane C: RNA alone, Lane OH: alkaline hydrolysis products, Lane T1: ribonuclease T1 products (G lane), Lanes 1–13: ribonuclease V1 products. Lane 1: No compound, Lanes 2–13: Two-fold increase of HTP **6** starting from 150 nM to a maximum of 300 μM. (Right) Secondary structure of RNA A with footprint of HTP **6** indicated.

EDTA·Fe–SV*Acr*R (**9**) (Fig. 3). Importantly, the cleavage patterns generated by these EDTA·Fe derivatives are nearly identical, although the concentrations necessary for efficient cleavage differ.

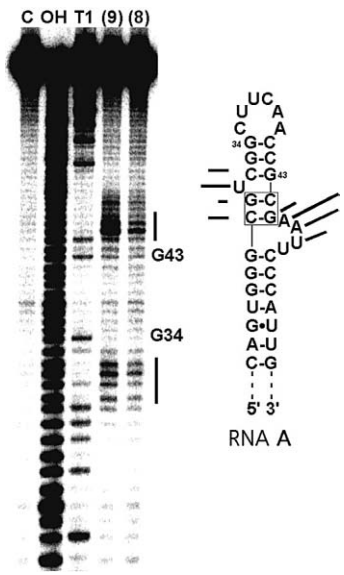

Fig. 3 Affinity cleavage of RNA A with HTPs **8** and **9**. (Left) Autoradiogram of polyacrylamide gel used to resolve affinity cleavage reactions. Lane C: RNA alone, Lane OH: alkaline hydrolysis products, Lane T1: ribonuclease T1 products (G lane), Lane (9); 10 μM HTP 9, Lane (8): 75 μM HTP **8**. (Right) Secondary structure of RNA A with cleaved nucleotides indicated by bars of varying lengths.

The similarity in cleavage patterns generated by **8** and **9** suggests that the change in intercalation domain from acridine to quinoline does not change the preferred binding polarity of the peptide with this RNA.

HTPs bind to sites in RNA predisposed to intercalation. The structural features that generate these intercalation "hot spots" in RNA continue to be defined.[9,12,13] For instance, we know that these sites consist of base paired steps adjacent to helix defects, such as bulges or internal loops.[4,9,12,13] However, how the defects allow the RNA to support HTP binding is not known. We have observed, as have others, that a bulge to the 3′-side of an intercalation site in duplex RNA facilitates binding of an intercalator.[4,9,13] Furthermore, we have shown that bulges on *both* strands to the 3′ side of an intercalation site are essential for HTP binding.[4] On the other hand, the extent to which HTP binding would be supported by bulges on the 5′ side of an intercalation site had not been evaluated. To address this issue, we used quinoline peptide **8** to assess HTP binding to two RNAs that differ in the positioning of bulges with respect to a potential intercalation site. We had shown previously that RNA **B**, which has bulges on both strands flanking a 5′-CpG-3′ intercalation site, supports binding of **9**.[4] Indeed, selective

binding is also observed for quinoline HTP **8** and this RNA (Fig. 4). However, no selective cleavage pattern is observed with **8** and RNA **C**, which has bulges flanking the intercalation site on the 5′ sides (Fig. 4). In addition, no selective HTP binding could be observed on RNA **C** using ribonuclease V1 footprinting (data not shown). Thus, not only is the quinoline HTP selective for a duplex with bulges, but it requires the bulged nucleotides to be properly positioned with respect to the intercalation site. These results underscore the ability of this class of compounds to selectively target certain RNA motifs over others of similar structure.

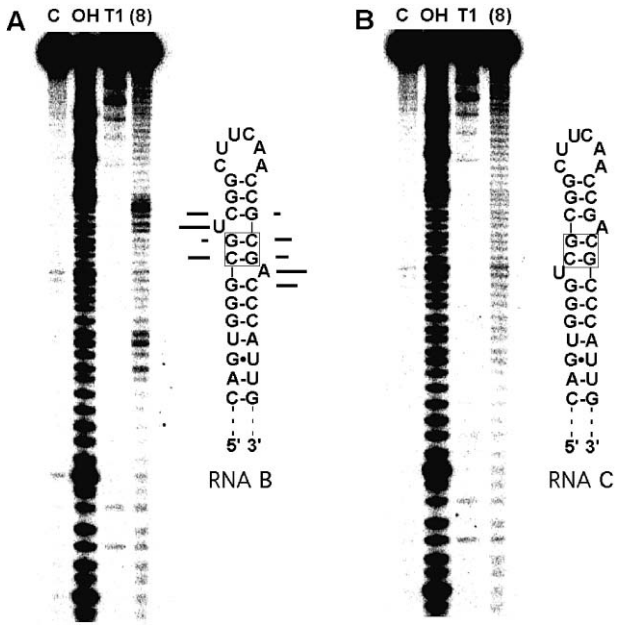

Fig. 4 Selective HTP binding requires 3' bulges flanking the intercalation site. (A) Affinity cleavage of RNA **B** with HTP **8**. The secondary structure of the RNA is shown with cleaved nucleotides indicated by bars whose lengths correspond to cleavage efficiency. (B) Affinity cleavage of RNA **C** with HTP **8**. Lane C: RNA alone, Lane OH: alkaline hydrolysis products, Lane T1: ribonuclease T1 products (G lane), Lane (8); 75 μM HTP **8**.

Analysis of structural data available from various RNA duplexes provides some insight into a possible source of this selectivity.[14] Considering a two base pair intercalation site in a canonical A-form RNA duplex, the nucleotide to the 3′-side on each strand stacks effectively above and below these base pairs. Alternatively, the nucleotides on each strand 5′ to the intercalation site stack onto these base pairs less extensively. The differential stacking of dangling bases located on either the 5′ or 3′ side of a terminal base pair in an A-form helix has also been used to explain why 3′ dangling nucleotides are much more effective at stabilizing duplex RNA than are 5′ dangling nucleotides.[15] It follows that bulges on the 3′ side of an intercalation site would disrupt the favorable stacking that stabilize the base pairs of the intercalation site to a greater degree than would bulged nucleotides to the 5′ side. This analysis is supported by structural data from an RNA duplex with two uridine bulges flanking a central 5′–CpG–3′ step on the 5′ side in each strand.[16] This structure shows minimal disruption in the stacking above and below the CpG. However, considering the base pairs on the opposite sides of the bulges (where the bulge is 3′ to the base pair), base stacking is substantially altered. Therefore, conformational changes necessary for threading intercalation to occur, including breaking the stack at the intercalation site and base pair opening, would be facilitated more effectively by 3′ bulges than 5′ bulges.

When considering the utility of a small molecule design for controlling RNA function *in vivo*, one must also consider the stability of the compound in living cells in addition to its RNA-binding properties. Our original HTP design made use of 9-anilinoacridines.[3,4,9,10] However, 9-anilinoacridines are known to decompose in the presence of millimolar concentrations of thiols.[17,18] Indeed, this degradation pathway may have limited the development of certain acridine-based drug candidates.[17] Therefore, acridine-containing HTPs may not have the stability necessary for *in vivo* or tissue culture applications. To evaluate the stability of these compounds directly, we incubated the HTP AbuSV*Acr*R (**7**) in buffered aqueous solution containing 1 mM dithiothreitol (DTT) at ambient temperature (Fig. 5A). The reaction was monitored by UV–visible spectroscopy as a function of time. Under these conditions, the 9-anilinoacridine chromophore (λ_{max} = 442 nm) is lost with a $k_{obs} = 1.5 \pm 0.4 \times 10^{-3}$ min^{-1}, corresponding to a $t_{1/2}$ = 7.6 h. The major product of the reaction was HPLC purified and analyzed by mass spectrometry (LC-MS). The mass of this adduct is consistent with attack at C9 by DTT, as observed by others with 9-anilinoacridine derivatives.[17,18] As expected, the DTT adduct binds poorly to RNA (data not shown). The decomposition observed for this compound under these conditions suggests that the acridine HTPs may have limited utility in cell-based assays given high intracellular thiol concentrations. However, in stark contrast to the acridine-containing peptide, quinoline HTP **6** remained unchanged under

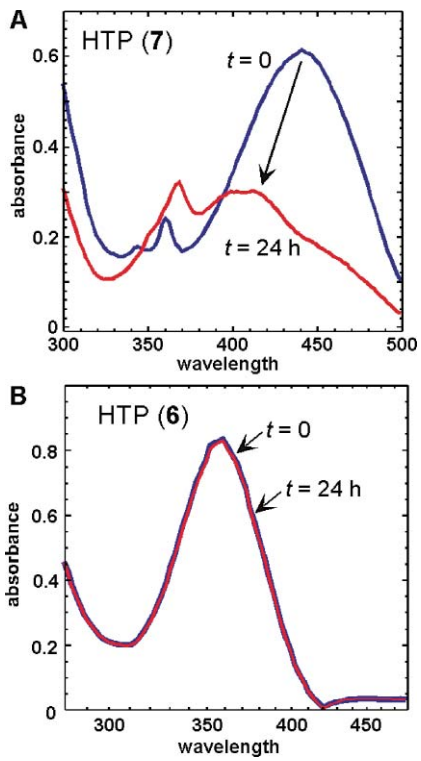

Fig. 5 Quinoline HTPs are resistant to thiolytic degradation. (A) Change in absorbance of acridine HTP **7** in aqueous buffer containing 1 mM DTT over 24 h at ambient temperature. (B) Absorbance of quinoline HTP **6** before and after the same treatment..

the aqueous DTT conditions described above for up to *two weeks* (Fig. 5B). The related 2-phenylquinoline compound[5] is also unaffected by this treatment (See Experimental section). Thus, although binding affinity is reduced by converting the acridine intercalation domain in HTPs to quinoline or 2-phenylquinoline, the greater stability in the presence of thiols is a clear advantage of these compounds for *in vivo* experiments.

In conclusion, a high-yielding synthesis to a quinoline amino acid has been developed for the generation of HTPs with minimal intercalation domains. This amino acid was used to prepare HTPs that bind selectively to duplex RNA sites placing the *N*-terminus in the minor groove. Importantly, HTPs are shown to have the ability to discriminate between RNA binding sites that differ only in the positioning of bulged nucleotides relative to the intercalation site. Finally, in contrast to their acridine counterparts, quinoline-containing HTPs are highly stable under physiologically relevant buffer conditions, making them excellent candidates for further development as regulators of intracellular RNA function.

Experimental

General methods

All reagents were obtained from commercial sources and were used without further purification unless noted otherwise. Glassware for all reactions was oven dried at 125 °C overnight and cooled in a dessicator prior to use. All reactions were carried out under an argon atmosphere and liquid reagents were introduced by oven-dried glass syringes. Tetrahydrofuran was distilled over sodium metal and benzophenone under an argon atmosphere while dichloromethane and acetonitrile were distilled over CaH_2. To monitor the progress of reactions, thin layer chromatography (TLC) was performed with Merck silica gel 60 F254 precoated plates, eluting with the solvents indicated. Yields were calculated for material which appeared as a single spot by TLC and homogeneous by ^{1}H NMR. Short and long wave visualization was performed with a Minerallight multiband ultraviolet lamp at 254 and 365 nm, respectively. Flash column chromatography was carried out using Mallinckrodt Baker silica gel 150 (60–200 mesh). ^{1}H and ^{13}C nuclear magnetic resonance spectra of pure compounds were acquired on VXL-300, VXR-500 or Inova-500 spectrometers at 500/300 and 125/75 MHz. Chemical shifts for proton NMR are reported in parts per million with reference to the solvent peak. The abbreviations s, d, dd, ddd, dt t, m, and br s correspond to singlet, doublet, doublet of doublets, doublet of doublet of doublets, doublet of triplet, triplet, multiplet, and broad singlet, in that order. High resolution chemical ionization (CI) and fast atom bombardment (FAB) spectra were recorded on a Finnigan MAT 95 mass spectrometer while electrospray ionization (ESI) spectra were recorded on a Finnigan LCQ ion-trap mass spectrometer. Distilled, deionized water was used for all aqueous reactions and dilutions. Reagents for DNA amplification, RNA synthesis/radioactive labeling, hydroxyl radical cleavage, and ribonuclease footprinting were purchased from Amersham Pharmacia Biotech: high purity solution NTP set (ATP/CTP/GTP/UTP, 100 mM), RNase-Free deoxyribonuclease I (DNase I), RNAguard ribonuclease inhibitor (porcine); New England Biolabs: T4 polynucleotide kinase (PNK); PerkinElmer Life Sciences: [γ-^{32}P]ATP (6000 Ci mmol^{-1}); Stratagene: Pfu Turbo DNA polymerase; USB: PCR nucleotide mix (dATP–dCTP–dGTP–dTTP, 10 mM) and shrimp alkaline phosphatase (SAP). All commercial reagents were used as purchased without further purification. Chemically synthesized deoxyribonucleic acids were prepared by the DNA/Peptide Core Facility at the University of Utah Health Sciences Center (HSC). Storage phosphor autoradiography was carried out and analyzed using Molecular Dynamics imaging screens, Typhoon 9400 phosphorimager and ImageQuant 5.2 software.

Meldrum's acid derivative (1). To methyl anthranilate (10.8 mL, 83.3 mmol) in triethyl formate (41.5 mL, 249.8 mmol) was added Meldrum's acid (6.04 g, 41.63 mmol). The reaction mixture turned yellow and formed a white precipitate immediately. The precipitate was melted at 70–80 °C for 45 min when TLC (85% $CHCl_3$–MeOH) indicated complete disappearance of Meldrum's acid. The reaction mixture was cooled to room temperature. The precipitate formed was filtered and washed with ethanol, and the solvent removed under reduced pressure to afford **1** (11.92 g, 94%) as a white solid. δ_H (500 MHz; $CDCl_3$) 8.69 (1 H, d, *J* 14.2), 8.06 (1 H, dd, *J* 8.3 and 1.5), 7.58 (1 H, dt, *J* 8.1, 7.6 and 1.5), 7.47 (1 H, d, *J* 8.3), 7.24 (1 H, dd, *J* 8.3 and 7.3), 3.96 (3 H, s), 1.69 (6 H, s). δ_C (75 MHz; $CDCl_3$) 166.7, 164.3, 164.1, 151.1, 139.9, 134.9, 132.5, 125.6, 118.4, 116.1, 105.1, 89.4, 53.1, 27.4; *m/z* (FAB) 306.0991 (M^+ + H. $C_{15}H_{16}NO_6$ requires 306.0978).

8-(Methoxycarbonyl)-4-(1*H*)-quinolone (2). Compound **1** (3.01 g, 9.87 mmol) was added to refluxing phenyl ether (30 mL) at 255 °C. The resulting brown solution was stirred at 255 °C for 30 min under argon when TLC (85% $CHCl_3$–MeOH) indicated complete disappearance of starting material. The solution was cooled to room temperature and directly loaded on a silica gel column. The phenyl ether was removed using 50% EtOAC–hexanes. The product was then eluted using 2–3% MeOH–$CHCl_3$ to afford the 4-quinolone ester **2** (1.68 g, 84%) as a tan colored solid. δ_H (300 MHz; $CDCl_3$) 8.61 (1 H, d, *J* 7.8), 8.35 (1 H, dd, *J* 7.6 and 1.0), 7.69 (1 H, dd, *J* 7.1 and 6.6), 7.34 (1 H, dd, *J* 7.9 and 7.6), 6.33 (1 H, d, *J* 7.3), 3.98 (3 H, s). δ_C (75 MHz; $CDCl_3$) 178.1, 168.1, 140.6, 138.2, 135.1, 132.8, 127.1, 122.3, 115.0, 111.1, 52.6. *m/z* (FAB) 204.0636 (M^+ + H. $C_{11}H_{10}NO_3$ requires 204.0661).

Methyl-4-bromo-quinoline-8-carboxylate (3). To a solution of PPh_3 (657 mg, 2.51 mmol) in freshly distilled acetonitrile (8 mL) was added *N*-bromosuccinimide (446 mg, 2.51 mmol). The resulting solution was stirred at room temperature for 30 min under argon. A solution of **2** (102 mg, 0.50 mmol) in chloroform (1 mL) was added to the above solution and the reaction mixture was heated at reflux for 30 min. TLC (50% EtOAc–hexanes) indicated complete conversion. The solvent was removed under reduced pressure. The residue was dissolved in chloroform, extracted twice with saturated $NaHCO_3$ and brine. The organic layer was dried over anhydrous Na_2SO_4, and the solvent was removed under reduced pressure. Purification by silica gel column chromatography (20% EtOAc–hexanes) afforded **3** (101 mg, 76%) as a white solid. δ_H (300 MHz; $CDCl_3$) 8.75 (1 H, d, *J* 4.6), 8.31 (1 H, dd, *J* 8.4 and 1.0), 8.00 (1 H, dd, *J* 7.1 and 1.2), 7.71 (1 H, d, *J* 4.6), 7.63 (1 H, t, *J* 7.8), 4.02 (3 H, s). δ_C (75 MHz; $CDCl_3$) 168.1, 150.9, 146.3, 134.5, 132.5, 131.2, 130.3, 127.1, 125.9, 53.0. *m/z* (CI) 265.9799 (M^+ + H. $C_{11}H_9BrNO_2$ requires 265.9817.

Methyl-4-(4′-methylaminoallyoxycarbamate)anilino-quinoline-8-carboxylate (4). To a solution of methyl-4-bromo-quinoline-8-carboxylate (**3**) (101 mg, 0.38 mmol) in freshly distilled acetonitrile (8 mL) was added a solution of allyl-4-aminobenzylamino-carbamate[3] (117 mg, 0.57 mmol) dissolved in freshly distilled acetonitrile (1 mL). The resulting solution was heated at reflux for 40 min. TLC (85% $CHCl_3$–MeOH) indicated complete conversion. The solvent was removed under reduced pressure. The residue was dissolved in chloroform and extracted with saturated $NaHCO_3$ and brine. The organic layer was dried over anhydrous Na_2SO_4, and the solvent was removed under reduced pressure. Purification by silica gel column chromatography (3% MeOH–$CHCl_3$) afforded **4** (131 mg, 89%) as a yellow solid. ^{1}H NMR (300 MHz; $CDCl_3$) δ (ppm): 8.39 (1 H, br s), 8.05 (1 H, d, *J* 7.1), 7.37–7.28 (5 H, m), 7.06 (2 H, d, *J* 7.3), 6.48 (1 H, br s), 5.94 (1 H, ddd, *J* 17.1, 10.7 and 5.5), 5.31 (1 H, d, *J* 17.3), 5.22 (1 H, d, *J* 10.3), 5.14 (1 H, br s), 4.61 (2 H, d, *J* 5.1), 4.36 (2 H, d, *J* 5.8), 3.99 (3 H, s). δ_C (125 MHz; DMSO-d_6) 169.58, 156.91, 151.73, 148.88, 146.24, 139.63, 136.28, 134.48, 133.58, 128.85, 125.24, 124.33, 123.39, 120.43, 117.67, 102.36, 65.08, 52.85, 44.13. *m/z* (FAB) 392.1612 (M^+ + H. $C_{22}H_{22}N_3O_4$ requires 392.1610).

4-(4′-Methylaminoallyoxycarbamate)anilino-quinoline-8-carboxylic acid (5). To a solution of **4** (109 mg, 0.28 mmol) in freshly distilled THF (2 mL), was added lithium hydroxide monohydrate (12 mg, 0.28 mmol) in water (1 mL). The resulting solution was stirred at room temperature under argon for 2 h. TLC (85 : 14 : 1 $CHCl_3$–MeOH–AcOH) indicated complete conversion. The reaction mixture was neutralized with 0.1 N HCl, the solvent was removed under reduced pressure. The residue was dissolved in CH_2Cl_2 and extracted with brine. The organic layer was dried over anhydrous Na_2SO_4, and the solvent was removed under reduced pressure. The residue was dried under vacuum to afford the carboxylic acid **5** (87 mg, 83%) as a yellow solid. δ_H (300 MHz; $CDCl_3$/CD_3OD) 8.58 (1 H, d, *J* 7.3), 8.42 (1 H, d, *J* 8.3), 8.14 (1 H, d, *J* 6.6), 7.61 (1 H, dd, *J* 8.1 and 7.8), 7.38–7.28 (5 H, m), 6.73 (1 H, d, *J* 6.8), 5.86 (1 H, ddd, *J* 17.3, 10.6 and 5.4), 5.25 (1 H, d, *J* 17.1), 5.15 (1 H, d, *J* 10.5), 4.53 (2 H, d, *J* 5.4), 4.33 (2 H, s). δ_C (125 MHz; DMSO-d_6) 167.63, 156.42, 154.23, 145.48, 140.57, 138.89, 136.37, 136.13, 133.91, 128.80, 128.55, 125.71, 125.18, 121.13, 118.29, 117.19, 100.77, 64.61, 43.55. *m/z* (CI) 378.1450 (M^+ + H. $C_{21}H_{20}N_3O_4$ requires 378.1454).

AbuSV*Quin*R (6). Peptide **6** was synthesized using Fmoc-protected amino acids (NovaBiochem) according to standard SPPS protocols. Rink Amide MBHA resin (NovaBiochem; 0.64 mmol g^{-1} loading, 50 mg, 0.032 mmol) was added to a 15 mL fritted-glass filter flask reactor equipped with a screw cap and Teflon stopcock. The resin was pre-swelled with DMF and shaken with 20% piperidine–DMF (5 mL) (2 × 15 min) on a Burrell Model 75 Wrist Action shaker to remove the Fmoc group. The resin was next washed with DMF, MeOH, and again with DMF. To a solution of Fmoc-Arg(Pbf)-OH (104 mg, 0.16 mmol, 5 eq), *N*-hydroxybenzotriazole HOBt (22 mg, 0.16 mmol, 5 equiv), and 2-(1*H*-Benzotriazole-1-yl)-1,1,3,3-tetramethyluronium hexafluorophosphate HBTU (61 mg, 0.16 mmol, 5 equiv) in DMF (3 mL) was added diisopropylethylamine (DIPEA, 56 μL, 0.32 mmol, 10 equiv) and this solution was added to the resin. The resin was agitated for ~5 h at ambient temperature, then washed consecutively with DMF and MeOH. After swelling in DMF, the resin was treated with 20% piperidine in DMF (2 × 15 min) to remove the *N*-terminal Fmoc protecting group, then washed. The subsequent alloc protected quinoline amino acid **5** (83 mg, 0.22 mmol) was coupled in an identical manner and the resin agitated for 24 h, washed with DMF and MeOH and then dried *in vacuo* overnight in preparation for removal of the allyloxycarbonyl (Alloc) group. Freshly distilled CH_2Cl_2 (3 mL) was added to the dry resin in the reactor under an argon atmosphere. Solutions of $Pd(PPh_3)_4$ (37 mg, 0.032 mmol, 1 equiv) and $PhSiH_3$ (95 μL, 0.77 mmol, 24 equiv) in CH_2Cl_2 (1 mL) were delivered *via* an oven-dried glass syringe and the reactor was shaken for 15 min, then repeated once more, to reveal a free amine. Following Alloc removal, the resin was washed with 0.5% DIPEA in DMF, 0.5% (w/v) sodium diethyldithiocarbamate in DMF, DMF, MeOH, and again DMF. The remaining amino acids, Fmoc-Val-OH, Fmoc-Ser(Trt)-OH and Fmoc-Abu-OH were then coupled according to the previously mentioned procedures. Upon removal of the *N*-terminal Fmoc group, the resin was prepared for cleavage of the peptide from the resin. Rinses with DMF, MeOH, AcOH, and finally MeOH were performed, and the reactor was placed under high vacuum overnight. The dry resin was then suspended in a "cleavage cocktail" solution of trifluoroaceticacid–triisopropylsilane–phenol–water (TFA–TIS–PhOH–H_2O; 88 : 5 : 5 : 2, 5 mL) and shaken for 5 h to effect cleavage from the resin and amino acid side chain deprotection. The resulting solution containing AbuSV*Quin*R (**6**) was collected and concentrated under reduced pressure. Ether precipitation of the residue, followed by extraction with water, and subsequent neutralization of the acidic aqueous layer with triethylamine gave the crude product. The crude product was HPLC-purified on a reverse phase C-18 column (4.6 × 250 mm, Vydac) and eluted after 7.9 min of a gradient of 0–60% CH_3CN in H_2O over 20 min with a flow rate of 1.0 mL min^{-1}. The purified compound was then lyophilized to dryness. Compound **6** was analyzed by ESI-MS by directly infusing into the instrument a solution of the peptide dissolved in a 1 : 1 mixture of CH_3CN–H_2O with 1% formic acid at a flow rate of 10 μL min^{-1}. Typical ESI-MS conditions utilized a capillary voltage of 6 V at 175 °C. Ultrapure nitrogen was used as a sheath gas at a flow rate of 60 (arb). Xcaliber software was used to run the instrument and analyze the data. ESI-MS calc'd mass for AbuSV*Quin*R ($C_{35}H_{49}N_{11}O_6$): 719.4, found $[M + H]^+$ 720.5 *m/z*, Molar extinction coefficient (ε) at λ_{max} = 359 nm was determined to be 11 700 $M^{-1}cm^{-1}$ for **6**.

EDTASV*Quin*R (8). Rink Amide MBHA resin (NovaBiochem; 0.64 mmol g^{-1} loading, 40 mg, 0.026 mmol) was added to a 15 mL fritted-glass filter flask reactor equipped with a screw cap and Teflon stopcock. The resin was pre-swelled with DMF and shaken with 20% piperidine–DMF (5 mL) (2 × 15 min) on a Burrell Model 75 Wrist Action shaker to remove the Fmoc group. The resin was next washed with DMF, MeOH, and again with DMF. Fmoc-Arg(Pbf)-OH and the Alloc-protected quinoline amino acid **5** were coupled in an identical manner as above followed by alloc deprotection and coupling of subsequent amino acids Fmoc-Val-OH and Fmoc-Ser(Trt)-OH. Following Fmoc deprotection and washings, ethylenediaminetetraacetic acid (EDTA) monoanhydride[19] (10 equiv), was dissolved in warm anhydrous DMF and added to the resin and the reactor was agitated overnight at ambient temperature. The resin was then

washed and dried under vacuum overnight followed by cleavage with TFA–PhOH–H_2O–TIPS (88 : 5 : 5 : 2) for 5 h at ambient temperature to effect cleavage from the resin and amino acid side chain deprotection. The resulting solution containing EDTASV*Quin*R (**8**) was collected and concentrated under reduced pressure. Ether precipitation of the residue, followed by extraction with water and neutralization with TEA gave the crude product. HPLC purification afforded pure **8**, which was analyzed by ESI-MS. ESI-MS calc'd mass for EDTASV*Quin*R ($C_{41}H_{56}N_{12}O_{12}$): 908.4, found $[M + H]^+$ 909.4 m/z.

Evaluation of stability of HTPs AbuSV*Acr*R, AbuSV*PhQ*R[5] and AbuSV*Q*R in DTT

To evaluate the stability of the three HTPs, ~20 nmol of each peptide was incubated in 10 mM DTT in Tris Buffer (pH = 7.3) (20 μL) for 24 h at room temperature. The three solutions were HPLC purified after 24 h and analyzed by mass spectrometry (LC-MS). In case of AbuSV*Acr*R, the major product was the DTT adduct formed by the attack of DTT at C9 of acridine, corresponding to m/z of 531.1 in ESI-MS. However, in the case of AbuSV*PhQ*R and AbuSV*Q*R, the peptides were intact and ESI-MS gave peaks of m/z 795.4 and 720.5 corresponding to $[M + H]^+$ for AbuSV*PhQ*R and AbuSV*Q*R respectively.

Kinetics of decomposition of AbuSV*Acr*R (7) in DTT

In order to evaluate the rate of decomposition of HTP **7** in DTT, the decrease in absorbance of **7** at λ_{max} = 442 nm (corresponding to λ_{max} of absorption of 9-anilino acridines) was followed as a function of time using a UV–vis spectrophotometer (Beckman DU 7400) in the presence of 1 mM DTT. The reaction was done under pseudo-first-order conditions where [**7**] = ~100 μM and [DTT] = 1 mM. The concentration of product formed was then plotted as a function of time, and the data were fitted to the equation: $[P]_t = [A]_0(1 - \exp(-k_{obs}t)$, where $[P]_t$ is the concentration of the product formed at time t, $[A]_0$ is the fitted reaction end-point and k_{obs} is the observed rate constant for decomposition of **7** in 1 mM DTT. The results are reported as the average and standard deviation for three different experiments. The $t_{1/2}$ of the reaction was then calculated using the average value of k_{obs}.

RNA synthesis and 5′-^{32}P labeling

RNAs **A** and **B** were generated by run-off transcription with T7 RNA polymerase according to published procedures.[4] RNA **C** was also transcribed in vitro according to the following protocol. First, an 86-nucleotide dsDNA PCR product was amplified from a chemically synthesized template using 25mer and 45mer DNA oligonucleotide primers. Sequences are as follows: 25mer, 5′-GAGCGTCAGTCTTCGTCCAGGCCGA-3′; 45mer, 5′-GCGAATTCTAATACGACTCACTCTCGGGCGG-TTTTTCGAAGCTTG-3′, the T7 promoter is underlined; 72mer template, 5′-GGGAGAGGAUACUACACGUGACAGUGGG-UCGCGGC UUCAACCGACGCCCAUUGCAUGUAGCAG-AAGCUUCCG-3′. The PCR product was extracted with phenol–chloroform, ethanol precipitated, and dissolved in 100 μL reaction volumes consisting of transcription buffer (80 mM HEPES, 25 mM $MgCl_2$, 2 mM spermidine, 30 mM dithiothreitol (DTT), pH 7.5), NTPs (8 mM), and RNase inhibitor (1 U μL^{-1}). Transcription was initiated with T7 RNA polymerase (0.03 mg mL^{-1}) and continued overnight at 40 °C. The reaction mixture was treated with RNase-Free DNase I (0.5 U μL^{-1}) and $CaCl_2$ (1 mM) for 1 h at 40 °C and purified on a 10.5% denaturing polyacrylamide gel. The transcribed RNA was visualized by UV shadowing, excised from the gel and eluted overnight *via* the crush and soak method. After filtration, the solution was extracted with phenol–chloroform, ethanol precipitated, and dissolved in water. The RNA concentration was determined by measuring the absorbance at 260 nm. For the preparation of 5′-^{32}P RNA, 30 pmol of the transcript was treated with SAP (0.1 U μL^{-1}) for 45 min at 37 °C, followed by heat inactivation of the enzyme for 15 min at 65 °C. The dephosphorylated RNA was immediately treated with T4 PNK (0.5 U μL^{-1}), [γ-^{32}P]-ATP (2 mCi mL^{-1}) and DTT (1 mM) and incubated for 45 min at 37 °C. Labeled RNA was gel purified, visualized by storage phosphor autoradiography, and isolated as previously described.

Quantitative RNase V1 footprinting

Dissociation constant for **6** on RNA **A** was obtained using RNase V1 under native conditions. Ligand–RNA complexes were formed by incubating increasing concentrations of the ligand with 5′-^{32}P labeled RNA (5 nM) for 15 min in reaction buffer (50 mM Bis-Tris·HCl, pH 7.0, 100 mM NaCl, 10 mM $MgCl_2$, and 10 μg mL^{-1} of yeast $tRNA^{Phe}$) at ambient temperature. Enzymatic digestions with RNase V1 (0.0001 U μL^{-1}) were carried out for 30 min at ambient temperature and quenched with hot, formamide loading buffer. Cleaved RNA was heat denatured and analyzed by 10.5% denaturing polyacrylamide gel electrophoresis. The cleavage efficiency at nucleotide(s) near the binding site was calculated by normalizing for any differential loading of each concentration of the ligand tested. For HTP **6** bound to RNA **A**, the footprint at A46 was monitored with respect to the V1-dependent constant band U54. The cleavage data for the RNA was converted to binding data for the ligand, assuming that the maximum cleavage efficiency corresponds to 0% occupancy and the minimum cleavage efficiency corresponds to 100% occupancy. The fraction of RNA bound by the ligand was plotted as a function of concentration, and the data were fitted to the equation: fraction RNA bound = [ligand]/([ligand] + K_d). The dissociation constant is reported as the average and standard deviation for three different experiments.

Affinity cleaving

HTPs **8** and **9** were incubated with 5′-^{32}P labeled RNAs (**A**, **B** or **C**) (5 nM) and two-fold excess of $Fe(NH_4)_2(SO_4)_2$ for 15 min in reaction buffer (50 mM Bis-Tris·HCl, pH 7.0, 100 mM NaCl, 10 mM $MgCl_2$, and 10 μg mL^{-1} of yeast $tRNA^{Phe}$) at ambient temperature. The resulting complexes were probed by initiating hydroxyl radical formation with the addition of hydrogen peroxide (0.01%) and DTT (5 mM). The reactions were allowed to proceed for 30 min at room temperature. The reactions were quenched by the addition of distilled, deionized water, followed by phenol–chloroform extraction and ethanol precipitation. Cleaved RNA was resuspended in formamide loading buffer, heat denatured, and analyzed by denaturing 10.5% polyacrylamide gel electrophoresis.

Acknowledgements

PAB acknowledges support from the National Institutes of Health (USA) (AI-49062).

References

1 J. Gallego and G. Varani, *Acc. Chem. Res.*, 2001, **34**, 836; W. D. Wilson and K. Li, *Curr. Med. Chem.*, 1990, **7**, 73; M. Froeyen and P. Herdewijn, *Curr. Top. Med. Chem.*, 2002, **2**, 1123.
2 N. W. Luedtke, Q. Li and Y. Tor, *Biochemistry*, 2003, **42**, 11391.
3 C. B. Carlson and P. A. Beal, *Bioorg. Med. Chem. Lett.*, 2000, **10**, 1979; C. B. Carlson and P. A. Beal, *Org. Lett.*, 2000, **2**, 1465.
4 B. D. Gooch and P. A. Beal, *J. Am. Chem. Soc.*, 2004, **126**, 10603.
5 M. Krishnamurthy, B. D. Gooch and P. A. Beal, *Org. Lett.*, 2004, **6**, 63.
6 W. A. Denny, G. J. Atwell and B. C. Baguley, *Anti-Cancer Drug Des.*, 1987, **2**, 263; G. J. Atwell, C. D. Bos, B. C. Baguley and W. A. Denny, *J. Med. Chem.*, 1988, **31**, 1048; G. J. Atwell, B. C. Baguley and W. A. Denny, *J. Med. Chem.*, 1989, **32**, 396.
7 H. Briehl, C. Lukosch and C. Wentrup, *J. Org. Chem.*, 1984, **49**, 2772.
8 M.-K. Jeon and K. Kim, *Tetrahedron Lett.*, 2000, **41**, 1943.
9 C. B. Carlson, M. Vuyisich, B. D. Gooch and P. A. Beal, *Chem. Biol.*, 2003, **10**, 663.
10 B. D. Gooch, M. Krishnamurthy, M. Shadid and P. A. Beal, *ChemBioChem*, 2005, **6**, 2247.
11 P. B. Dervan, *Science*, 1986, **232**, 464.
12 N. K. Tanner and T. R. Cech, *Nucleic Acids Res.*, 1985, **13**, 7741; N. K. Tanner and T. R. Cech, *Nucleic Acids Res.*, 1985, **13**, 7759.
13 J. M. Kean, S. A. White and D. E. Draper, *Biochemistry*, 1985, **24**, 5062; S. A. White and D. E. Draper, *Biochemistry*, 1989, **28**, 1892; S. A. White and D. E. Draper, *Nucleic Acids Res.*, 1987, **15**, 4049.
14 C. Dock-Bregeon, B. Chevrier, A. Podjarny, D. Moras, J. S. deBear, G. R. Gough, P. T. Gilham and J. E. Johnson, *Nature*, 1988, **335**, 375.
15 J. Isaksson and J. Chattopadhyaya, *Biochemistry*, 2005, **44**, 5390.
16 Y. Xiong, J. Deng, C. Sudarsanakumar and M. Sundaralingam, *J. Mol. Biol.*, 2001, **313**, 573.
17 M. N. Khan and L. Malspeis, *J. Org. Chem.*, 1982, **47**, 2731; P. Kestell, J. W. Paxton, L. G. C. Robertson, P. C. Evans, R. A. Dormer and B. C. Baguley, *Drug Metab. Drug Interact.*, 1988, **6**, 328.
18 W. R. Wilson, B. F. Cain and B. C. Baguley, *Chem.-Biol. Interact.*, 1977, **18**, 163; B. F. Cain, W. R. Wilson and B. C. Baguley, *Mol. Pharmacol.*, 1976, **12**, 1027.
19 Y. W. Ebright, Y. Chen, P. S. Pendergrast and R. H. Ebright, *Biochemistry*, 1992, **31**, 10664.